Neuron, Vol. 32, 997–1012, December 20, 2001, Copyright ©2001 by Cell Press

# Assigning the Positional Identity of Spinal Motor Neurons: Rostrocaudal Patterning of Hox-c Expression by FGFs, Gdf11, and Retinoids

**Jeh-Ping Liu,[1,3] Ed Laufer,[2] and Thomas M. Jessell[1,4]**
[1] Howard Hughes Medical Institute
Department of Biochemistry
and Molecular Biophysics
Columbia University
701 West 168th Street
New York, New York 10032
[2] Department of Genetics and Development
Columbia University
701 West 168th Street
New York, New York 10032
[3] Department of Neuroscience
University of Virginia School of Medicine
Lane Road Extended
Charlottesville, Virginia 22908

## Summary

**Subclasses of motor neurons are generated at different positions along the rostrocaudal axis of the spinal cord. One feature of the rostrocaudal organization of spinal motor neurons is a position-dependent expression of *Hox* genes, but little is known about how this aspect of motor neuron subtype identity is assigned. We have used the expression profile of Hox-c proteins to define the source and identity of patterning signals that impose motor neuron positional identity along the rostrocaudal axis of the spinal cord. We provide evidence that the convergent activities of FGFs, Gdf11, and retinoid signals originating from Hensen's node and paraxial mesoderm establish and refine the Hox-c positional identity of motor neurons in the developing spinal cord.**

## Introduction

Developing neurons possess positional identities that permit them to form selective connections with target cells. In the vertebrate central nervous system (CNS), neurons acquire their positional identity in response to the spatially restricted actions of extrinsic signaling factors. Typically, these factors act by inducing the expression of transcription factors that impose the identity of their neuronal progeny. In this view, the position that a progenitor cell occupies in the neural tube is a critical determinant of its later neuronal identity. Details of the signaling pathways by which neurons acquire positional identity, however, remain poorly defined.

The steps that link neuronal position and identity have been explored in the developing spinal cord. Here, neuronal patterning appears to be regulated by signaling systems that operate along the dorsoventral (D-V) and rostrocaudal (R-C) axes of the neural tube (Lumsden and Krumlauf, 1996; Tanabe and Jessell, 1996). The D-V pattern of neuronal generation depends on bone morphogenetic protein (BMP) and Hedgehog signaling (Briscoe and Ericson, 2001; Lee and Jessell, 1999). The secretion of Sonic hedgehog (Shh) from the notochord and floor plate is critical for the patterning of ventral cell types (Briscoe and Ericson, 2001; Patten and Placzek, 2000). Shh signaling controls ventral neuronal fates by regulating the expression profile of homeodomain (HD) proteins that determine the positional identity of postmitotic neurons (Briscoe and Ericson, 2001).

The mechanisms that establish the identity of neuronal subtypes along the R-C axis of the spinal cord are less well defined. Interneuron subclasses are typically generated along the entire R-C extent of the spinal cord, whereas developing motor neurons (MNs) exhibit marked R-C differences in identity. Two major distinctions in the R-C identity of spinal MNs have been defined through studies of their position, axon trajectory, and pattern of muscle innervation (Landmesser, 2001). One is the allocation of MNs to discontinuous columnar divisions: thus lateral motor column (LMC) neurons are generated only at limb levels, whereas visceral MNs are generated at thoracic levels (Hollyday, 1980a, 1980b; Landmesser, 1978a, 1978b). A second distinction is evident in the formation of pools of MNs that occupy distinct R-C positions within the LMC, each pool innervating a different target muscle (Hollyday, 1980a; Landmesser, 1978b). These distinctions in the R-C positional identity of MNs have been linked to the expression of transcription factors (Jessell, 2000). Columnar subclasses of MNs can be delineated by the profile of LIM-HD protein expression (Tsuchida et al., 1994), and MN pools can be recognized by the expression of ETS proteins (Lin et al., 1998). Furthermore, genetic studies have begun to provide evidence that LIM-HD and ETS proteins regulate the subtype identity and pattern of connectivity of developing MNs (Sharma et al., 1998; Kania et al., 2000; S. Arber, personal communication).

An additional R-C distinction in MN identity, superimposed upon programs of column and pool organization is evident as a graded positional value that is linked to the topographic projections of somatic and visceral MNs within their target fields (Forehand et al., 1994; Laskowski and Sanes, 1987). The only known molecular correlate of this graded R-C positional identity of MNs is the expression of members of the *Hox* gene family (Belting et al., 1998; Ensini et al., 1998; Lance-Jones et al., 2001). Moreover, there is emerging functional evidence that *Hox* genes control the projection patterns of motor axons. Inactivation of members of the *Hox-c* and *Hox-d* gene clusters leads to alterations in motor innervation of specific muscles in the limb (Carpenter et al., 1997; de la Cruz et al., 1999; Tiret et al., 1998), and in the developing hindbrain, *Hox-a* and *Hox-b* genes control the identity and axonal trajectory of cranial MNs (Bell et al., 1999; Gavalas et al., 1997; Jungbluth et al., 1999; Studer et al., 1996).

Despite evidence for Hox-based R-C positional differences in MN identity, the extrinsic signals that control *Hox* gene expression in the spinal cord have not been defined. Grafting studies in chick embryos have provided evidence that the positional identity of spinal MNs,

[4] Correspondence: tmj1@columbia.edu

as well as the pattern of *Hox* gene expression, can be respecified soon after neural tube closure by signals derived from the paraxial mesoderm (Ensini et al., 1998). Similarly, in the hindbrain, signals from the paraxial mesoderm have been implicated in the regulation of *Hox* gene expression (Grapin-Botton et al., 1997; Itasaki et al., 1996). Nevertheless, it remains unclear whether signals from the paraxial mesoderm are sufficient to establish the R-C positional identity of MNs. In the lumbar spinal cord, for example, the developmental profile of *Hox-d* gene expression cannot easily be accounted for by signals from the paraxial mesoderm (Lance-Jones et al., 2001).

In this study, we have examined the factors that establish the graded R-C positional identity of MNs, through an analysis of Hox-c protein expression. Our findings indicate that the convergent activities of three classes of extrinsic signals—FGFs, Gdf11, and retinoids—appear to be involved in establishing the Hox-c positional identity of spinal MNs.

## Results

### Rostrocaudal Expression of Hox-c Proteins in the Developing Spinal Cord

To generate markers that define the positional identity of MNs along the R-C axis of the developing spinal cord, we raised antibodies against Hoxc5, Hoxc6, Hoxc8, Hoxc9, and Hoxc10. These antibodies were used to define the temporal and spatial pattern of Hox-c expression in the embryonic chick spinal cord.

#### *Temporal Pattern*

The neural expression of Hox-c proteins was first detected at HH stage 14, when low levels of Hoxc8, Hoxc9, and Hoxc10 were expressed in a few cells in the caudal neural tube (data not shown). From HH stages 16 to 22, the peak period of MN generation (Hollyday and Hamburger, 1977), the expression of Hoxc5, Hoxc6, Hoxc8, Hoxc9, and Hoxc10 was restricted primarily to Isl1(2)$^+$, HB9$^+$ MNs (Figure 1A; data not shown). Newly differentiated MNs are located medially, and these neurons lacked Hox-c expression (Figure 1A; data not shown), indicating that the onset of Hox-c expression occurs after MNs have left the cell cycle. Hox-c expression in MNs persisted at HH stage 24, close to the end of MN generation, and at this stage expression was also detected in other cell types (Figure 1C). From HH stages 24 to 28, the expression of Hox-c proteins, notably Hoxc8 and Hoxc9, became restricted to columnar subsets of MNs (Supplemental Figure S1 at http://www.neuron.org/cgi/content/full/32/6/997/DC1).

#### *Spatial Pattern*

We next analyzed the pattern of Hox-c expression in MNs at different R-C levels of the spinal cord, from HH stages 16 to 24. Over this period, different Hox-c proteins were expressed in restricted R-C domains. At HH stage 24, Hoxc5 was detected throughout the cervical spinal cord, with a posterior limit of expression in the rostral brachial spinal cord (Figures 1B and 1C). Hoxc6 was detected from caudal cervical levels into the brachial region (Figures 1B and 1C). Hoxc8 was detected from the mid-brachial to the mid-thoracic levels (Figures 1B and 1C). Hoxc9 was detected from caudal brachial through thoracic levels (Figures 1B and 1C). Hoxc10 was detected in the lumbar spinal cord (Figures 1B and 1C). These results extend previous studies (Belting et al., 1998; Ensini et al., 1998), and provide evidence that developing spinal MNs exhibit R-C identities that can be defined by their Hox-c expression profile.

### Early Specification of the Neural Pattern of Hox-c Expression

To examine how the R-C identity of spinal MNs is established, we assayed the timing of specification of Hox-c expression in chick neural tissue in vitro. We first analyzed the profile of Hox-c expression in neural explants isolated from different R-C positions of the neural tube in 14 to 15 somite stage (s) embryos. Ventral neural tissue positioned caudal to the most recently formed somites and rostral to Hensen's node (HN) was isolated together with prospective or definitive floor plate cells, to provide a source of Shh to initiate spinal MN generation (Ericson et al., 1996). Neural tissue was subdivided into five R-C domains, each domain was cultured in vitro for 66 hr (to the equivalent of HH stages 24–25), and then assayed for Hox-c expression (Figure 2A). The positional fate of neural cells in these five domains was determined in vivo (see Experimental Procedures).

Cells in neural explants fated to populate caudal cervical levels expressed Hoxc6, but not other Hox-c proteins (Figure 2B). Cells in neural explants fated to give rise to rostral brachial levels expressed Hoxc6 and low levels of Hoxc8, but not Hoxc9 or Hoxc10 (Figure 2B). Neural explants fated to give rise to caudal brachial levels contained many Hoxc6$^+$ and Hoxc8$^+$ cells, a few Hoxc9$^+$ cells, but no Hoxc10$^+$ cells (Figure 2B). Neural explants fated to give rise to rostral thoracic levels expressed fewer Hoxc6$^+$ and many Hoxc8$^+$ and Hoxc9$^+$ cells, but no Hoxc10$^+$ cells (Figure 2B). Cells in neural explants fated to populate caudal thoracic levels of the neural tube expressed low levels of Hoxc6, higher levels of Hoxc8 and Hoxc9, but not Hoxc10 (Figure 2B). These caudal thoracic explants contain Hoxc6$^+$ and Hoxc8$^+$ cells, even though the spinal cord at this level in vivo lacks expression of both proteins (Figures 1B and 1C), an issue we return to below. No expression of Hoxc5 was detected in any of these explants (data not shown). Many Hox-c$^+$ cells were MNs, as assessed by coexpression of Isl1(2), although Hox-c proteins were also detected in other cell types, as in vivo (Figure 2C; data not shown). The expression of each of these Hox-c proteins was first detected between 24 hr–48 hr (data not shown), a timing consistent with their onset of expression in vivo. Thus, neural Hoxc6 to Hoxc10 expression patterns in chick embryos are specified by the 14s stage.

We also monitored the Hox-c profile of MNs generated in neural plate tissue isolated from 5s, 10s, and 20s (HH stages 8+, 10, and 13+) embryos (Figures 3A, 3C, and 3E). Ventral neural tissue located anterior to HN in 5s embryos is fated to populate rostral cervical levels, and none of the MNs generated in these explants expressed Hoxc6, Hoxc8, Hoxc9, or Hoxc10 (Figures 3A and 3B). Ventral neural tissue isolated from the region anterior to HN in 10s embryos is fated to populate rostral brachial levels, and MNs in these explants expressed Hoxc6 and Hoxc8, but not Hoxc9 or Hoxc10 (Figures 3C and 3D; data not shown). Ventral neural tissue isolated from the region anterior to HN in 20s embryos is fated to populate

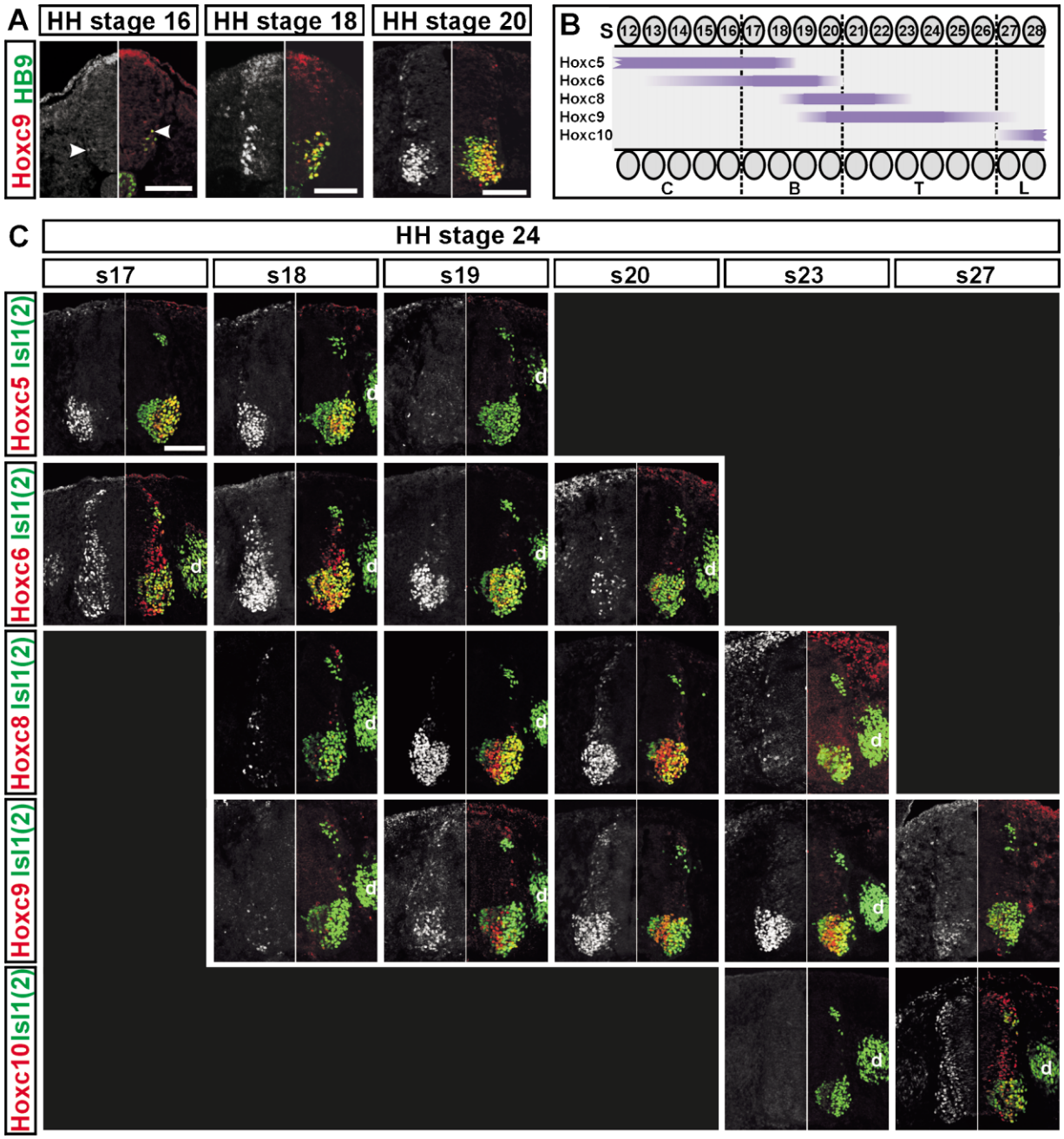


Figure 1. Hox-c Expression in Developing Spinal MNs

(A) Hoxc9 and HB9 expression in the spinal cord of HH stage 16–20 embryos. Arrowheads indicate Hoxc9$^+$ cells. Left side shows expression of Hoxc9, and right side Hoxc9 (red) and HB9 (green).

(B) R-C domains of Hoxc5 to Hoxc10 in the spinal cord of HH stage 24 embryos. Numbers in circles indicate somite level. C = cervical, B = brachial, T = thoracic, and L = lumbar levels.

(C) Expression of Hoxc5 to Hoxc10 at different levels of HH stage 24 embryos. Left side shows individual Hox-c proteins, and right side Hox-c (red) and Isl1(2) (green). "d" indicates dorsal root ganglion.

Scale bar: 100 μm.

rostral lumbar levels, and MNs generated in these explants expressed Hoxc9 and Hoxc10, but not Hoxc6 or Hoxc8 (Figures 3E and 3F). No expression of Hoxc5 was detected in these explants (Figures 3D, 7A, and data not shown). Thus, with the exception of Hoxc5, the R-C profile of Hox-c expression in MNs and other cell types appears to be specified soon after neural plate formation.

### Induction of Neural Hox-c Expression by Hensen's Node

The early specification of neural Hox-c pattern led us to examine the origin of signals that establish this aspect of MN positional identity. Previous studies have provided evidence that the pattern of Hox expression is modifiable around the time of neural tube closure (Ensini et al., 1998; Lance-Jones et al., 2001). We reasoned that

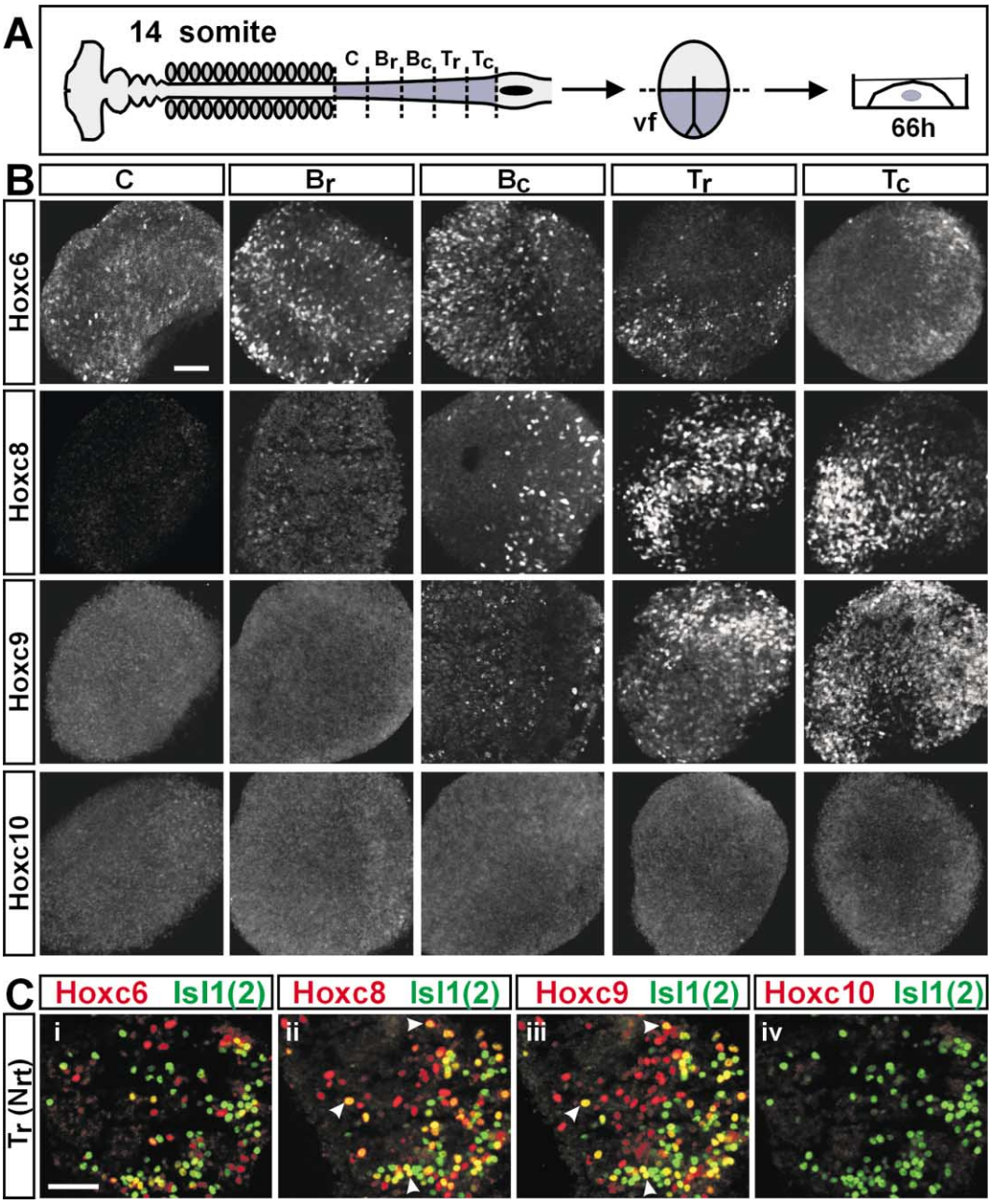


Figure 2. Expression of Hox-c in Neural Explants In Vitro

(A) Cells in neural tissue caudal to the somites and rostral to HN in 14s embryos populate cervical to thoracic regions of the spinal cord. (C = cervical, $B_r$ = rostral brachial, $B_c$ = caudal brachial, $T_r$ = rostral thoracic, $T_c$ = caudal thoracic). Ventral neural tissue including the floor plate (vf) was cultured for 66 hr.

(B) Expression of Hoxc6 to Hoxc10 in explants from (A).

(C) A $T_r$ ($N_{rt}$) explant generates Hoxc$^+$, Isl1(2)$^+$ cells. Panels i and iv are the same section labeled with Hoxc6, Hoxc10, and Isl1(2). Panels ii and iii are the same section labeled with Hoxc8, Hoxc9, and Isl1(2). Arrowheads indicate Hoxc8$^+$, Hoxc9$^+$ MNs.

Scale bar: 50 μm.

neural plate tissue fated to give rise to rostral cervical levels, and lacking expression of Hoxc5 to Hoxc10 in vitro (Figures 3A and 3B), might still be competent to respond to extrinsic signals that impose a more caudal Hox-c identity. We therefore used ventral neural explants isolated from the rostral cervical level of 5s to 6s embryos (termed $N_{rc}$ explants) (Figures 3A and 3B) in assays to define the source of Hox-c patterning activity. We also assayed the coexpression of Hox-c and Isl1(2) proteins to test whether the Hox-c expression pattern reflects MN positional identity and, in addition, determined the total number of Isl1(2)$^+$ MNs (Table 1).

From HH stage 6 onward, prospective spinal cord cells lie close to the rostral primitive streak and HN

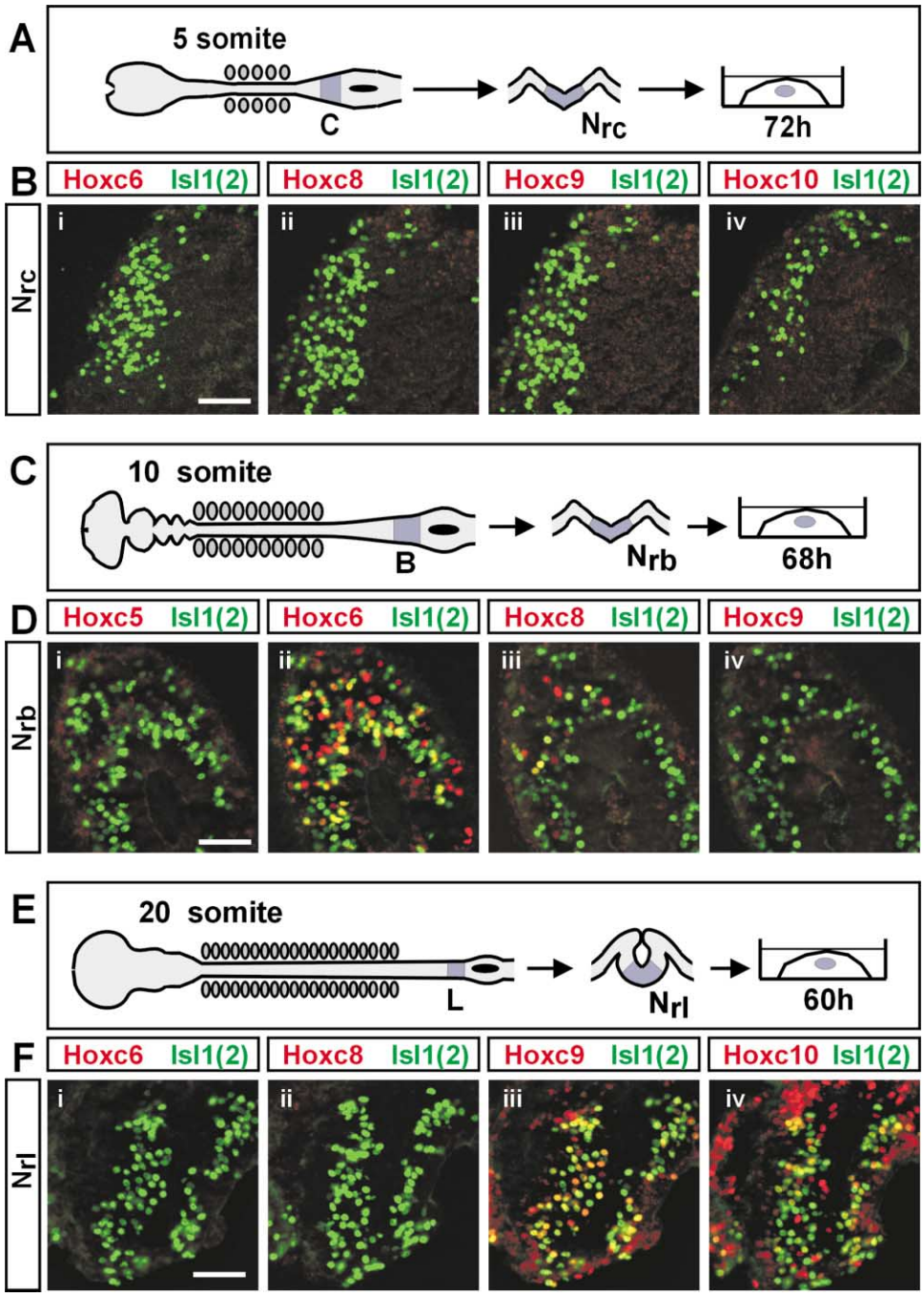


Figure 3. Hoxc6 to Hoxc10 Expression Is Specified at Neural Plate Stages

(A) Neural tissue located rostral to HN in 5s embryos populates rostral cervical levels of the spinal cord. Ventral neural plate ($N_{rc}$) tissue was cultured for 72 hr.

(B) $N_{rc}$ explants do not express Hoxc6 to Hoxc10. Panels ii and iii are the same section labeled with Hoxc8, Hoxc9 and Isl1(2).

(C) Neural tissue located rostral to HN in 10s embryos populates rostral brachial levels. Ventral neural plate ($N_{rb}$) tissue was cultured for 68 hr.

(D) $N_{rb}$ explants cultured in vitro express Hoxc6 and Hoxc8. Panels i and ii are the same section labeled with Hoxc5, Hoxc6, and Isl1(2). Panels iii and iv are the same section labeled with Hoxc8, Hoxc9, and Isl1(2).

(E) Neural tissue located rostral to HN in 20s embryos populates rostral lumbar levels. Ventral neural plate ($N_{rl}$) tissue taken from this region was cultured for 60 hr.

(F) $N_{rl}$ explants express Hoxc9 and Hoxc10. Panels i and iii are the same section labeled with Hoxc6, Hoxc9 and Isl1(2). Panels ii and iv are the same section labeled with Hoxc8, Hoxc10, and Isl1(2).

Scale bar: 50 μm.

Table 1. Motor Neuron Number in Neural Explants Exposed to Different Factors

| Explants + Reagents | Isl1 (2)$^+$ Cells/Section |
|---|---|
| $N_{rc}$ | 58 ± 11 |
| $N_{rc}$ + Fgf2 5 ng/ml | 114 ± 15 |
| $N_{rc}$ + Fgf2 25 ng/ml | 153 ± 11 |
| $N_{rc}$ + Fgf2 125 ng/ml | 184 ± 16 |
| $N_{rc}$ + Fgf2 625 ng/ml | 50 ± 4 |
| $N_{rc}$ + 5sHN | 146 ± 15 |
| $N_{rc}$ + 15sHN | 45 ± 7 |
| $N_{rc}$ + 15sHN + SU5402 12.5 M | 46 ± 18 |
| $N_{rc}$ + Gdf8 10 ng/ml | 33 ± 3 |
| $N_{rc}$ + Fgf2 25 ng/ml + Gdf8 10 ng/ml | 143 ± 22 |
| $N_{rc}$ + Gdf8 40 ng/ml | 43 ± 8 |
| $N_{rc}$ + Fgf2 25 ng/ml + Gdf8 40 ng/ml | 102 ± 9 |
| $N_{rc}$ + RA 0.1 M | 114 ± 22 |
| $N_{rt}$ | 98 ± 8 |
| $N_{rt}$ + Fgf2 5 ng/ml | 209 ± 44 |
| $N_{rt}$ + Gdf8 5 ng/ml | 102 ± 15 |
| $N_{rt}$ + RA 0.1 M | 154 ± 12 |

Isl1(2)$^+$ MNs were counted in sections of neural explants. Each value represents Isl1(2)$^+$ cells/section from 2 to 4 explants (mean ± SEM).

(Mathis et al., 2001; Schoenwolf, 1992), leading us to examine whether signals from these axial tissues are involved in the induction of neural Hox-c expression. Cells in $N_{rc}$ explants grown in conjugate with HN tissue (see Experimental Procedures) were induced to express Hoxc6, Hoxc8, Hoxc9, and Hoxc10, but not Hoxc5 (Figure 4; data not shown). The precise profile of Hox-c expression depended on the developmental stage at which HN was isolated, and by inference the R-C position of HN. HN tissue derived from 5s to 6s embryos induced ~50 Hoxc6$^+$ cells (Hox-c$^+$ cell number/10 μm section), but no Hoxc8$^+$, Hoxc9$^+$, or Hoxc10$^+$ cells (Figure 4). HN tissue derived from 10s to 11s embryos induced ~80 Hoxc6$^+$ cells, 20 to 40 Hoxc8$^+$ and Hoxc9$^+$ cells, but no Hoxc10$^+$ cells (Figure 4). HN tissue derived from 14s to 15s embryos induced fewer (~30) Hoxc6$^+$ cells, slightly more (~30) Hoxc8$^+$ cells, many more (~120) Hoxc9$^+$ cells, and ~10 Hoxc10$^+$ cells (Figure 4). HN tissue from 19s to 20s embryos induced ~10 Hoxc6$^+$ cells, ~30 Hoxc8$^+$ cells, and additional Hoxc9$^+$ and Hoxc10$^+$ cells (Figure 4). In all instances, many induced Hox-c$^+$ cells were MNs, as assessed by coexpression of Isl1(2) (Table 1; data not shown). These findings provide evidence that signals from older and progressively more caudally positioned HN tissue induce a correspondingly more caudal profile of Hox-c expression.

We also examined whether tissues adjacent to HN induce neural Hox-c expression. $N_{rc}$ explants were cultured together with caudal paraxial mesoderm, notochord, or ventral neural tissue isolated from 15s quail embryos. Newly formed notochord tissue at caudal thoracic level induced a few Hoxc6$^+$ cells, but did not induce Hox5$^+$, Hoxc8$^+$, Hoxc9$^+$, or Hoxc10$^+$ cells (data not shown). In contrast, older notochord tissue at rostral thoracic levels did not induce expression of Hox-c proteins (data not shown). Neither paraxial mesoderm nor ventral neural tube tissue induced expression of Hox-c proteins (data not shown). Thus, Hox-c-inducing activity is concentrated in HN, but is also expressed transiently in the notochord, a derivative of HN.

### Concentration-Dependent Induction of Hox-c Expression by FGFs

Several fibroblast growth factor (FGF) genes, including *Fgf2*, *Fgf3*, *Fgf4*, and *Fgf8*, are expressed in HN and in the adjacent primitive streak (Crossley and Martin, 1995; Mahmood et al., 1995a; Niswander and Martin, 1992; Riese et al., 1995), leading us to analyze the Hox-c-inducing activity of FGFs. *Fgf8* is expressed in HN, primitive streak, and the tail bud over the time that the spinal Hox-c expression pattern is established, and the level of expression of *Fgf8* in HN and tail bud appeared to increase from the 6s to16s stages (Supplemental Figure S2 at http://www.neuron.org/cgi/content/full/32/6/997/DC1). In 16s stage embryos, *Fgf8* expression was also detected in caudal regions of the notochord (Supplemental Figure S2). We therefore tested whether FGF8, or other FGFs with similar activity, mimic the ability of HN to induce Hox-c expression in $N_{rc}$ explants.

FGF8 activity requires heparin as a cofactor (Mahmood et al., 1995b; Storey et al., 1998; our observations). We therefore examined the Hox-c inductive ability of FGF8-adsorbed heparin beads, when grown in contact with $N_{rc}$ explants for 72 hr. Heparin beads soaked in 11 μg/ml FGF8 induced expression of Hoxc6 in cells close to the bead, but did not induce Hoxc8, Hoxc9 ,or Hoxc10 (data not shown). Heparin beads soaked with 33 μg/ml FGF8 induced Hoxc6, Hoxc8, and Hoxc9 (data not shown), and heparin beads soaked with 100 μg/ml FGF8 induced Hoxc6 in distant cells, induced Hoxc8 and Hoxc9 in cells nearer to the beads, and induced Hoxc10 in cells adjacent to the beads (Supplemental Figure S3 on *Neuron* website). Hoxc5 was not detected in any of these conditions (data not shown). These results provide evidence that FGF8 can induce Hox-c expression in $N_{rc}$ explants, and suggest that the profile of Hox-c expression varies with the concentration of FGF8.

To examine the influence of FGFs on Hox-c expression more quantitatively, we exposed $N_{rc}$ explants to defined concentrations of FGF2, an FGF that mimics the activity of FGF8 in chick neural plate tissue (Muhr et al., 1999), and exhibits signaling activity in soluble form in the absence of heparin (Roghani et al., 1994). Exposure of $N_{rc}$ explants to 5 ng/ml FGF2 induced ~20 Hoxc6$^+$, Isl1(2)$^+$ MNs (mean values/10 μm section), but no Hoxc8$^+$, Hoxc9$^+$, or Hoxc10$^+$ MNs (Figure 5A). Exposure of $N_{rc}$ explants to 25 ng/ml FGF2 induced 17 Hoxc6$^+$, Isl1(2)$^+$ MNs; 25 Hoxc8$^+$, Isl1(2)$^+$ MNs; 36 Hoxc9$^+$, Isl1(2)$^+$ MNs; but no Hoxc10$^+$, Isl1(2)$^+$ MNs (Figure 5A). Exposure of $N_{rc}$ explants to 125 ng/ml FGF2 induced 4 Hoxc6$^+$, Isl1(2)$^+$ MNs; 57 Hoxc8$^+$, Isl1(2)$^+$ MNs; 97 Hoxc9$^+$, Isl1(2)$^+$ MNs; and 5 Hoxc10$^+$, Isl1(2)$^+$ MNs (Figure 5A). Exposure of $N_{rc}$ explants to 625 ng/ml FGF2 induced 1 Hoxc6$^+$, Isl1(2)$^+$ MN; 1 Hoxc8$^+$, Isl1(2)$^+$ MN; 20 Hoxc9$^+$, Isl1(2)$^+$ MNs; and 26 Hoxc10$^+$, Isl1(2)$^+$ MNs (Figure 5A). FGF2 failed to induce Hoxc5 at these concentrations (data not shown; Figure 7C). These results provide evidence that the FGF8/FGF2 class of FGFs mimic the ability of HN to induce patterned Hox-c expression, and indicate that FGFs act in a concentration-dependent manner that appears to reflect the age- and position-dependent signaling activity of HN.

To test if the induction of neural Hox-c expression by HN requires FGF signaling, we used SU5402, an effective inhibitor of FGF receptor 1 (FGFR1) activity (Moham-

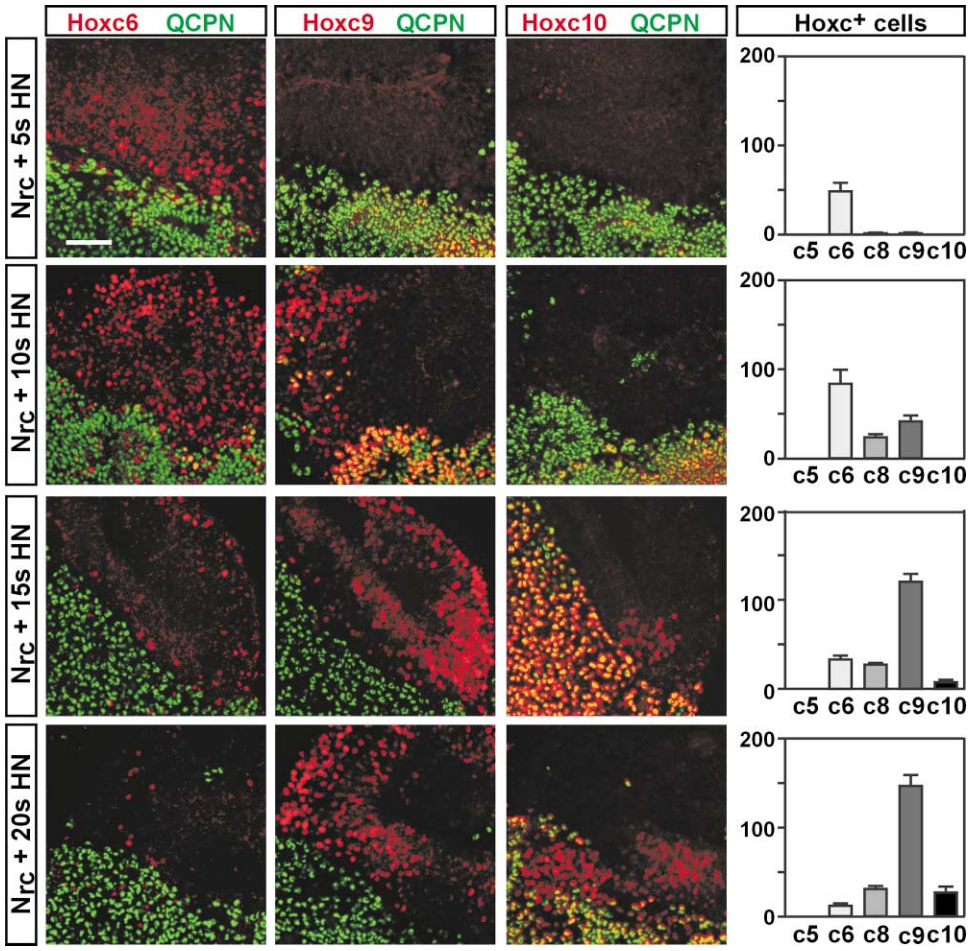


Figure 4. Induction of Neural Hox-c Expression by Hensen's Node

Coculture of HN tissue from 5s–20s quail embryos with $N_{rc}$ explants induces the expression of Hoxc6 to Hoxc10 proteins, but not Hoxc5. Scale bar: 50 μm.

madi et al., 1997; Muhr et al., 1999; Streit et al., 2000; Wilson et al., 2000). Conjugates of chick $N_{rc}$ explants and 15s quail HN tissue were grown in the presence of SU5402. The induction of neural Hoxc8, Hoxc9, and Hoxc10 expression by 15s quail HN was completely blocked by 5 μM SU5402 (data not shown). At this concentration, neural expression of Hoxc6 was not completely eliminated, but 12.5 μM SU5402 completely blocked expression of Hoxc6 as well as of Hox8, Hoxc9, and Hoxc10 (Figure 5B). The generation of Isl1(2)$^+$ MNs in these neural explants was not affected by SU5402 (Figure 5B, Table 1). These results provide evidence that the expression of Hoxc6 to Hoxc10 in MNs depends on FGF signals provided by HN.

### An Accessory Role for Gdf11 in Patterning Neural Hox-c Expression

The high FGF concentration needed to induce a caudal profile of neural Hox-c expression prompted us to examine whether FGFs account completely for the Hox-c patterning activity of HN. Gdf11, a member of the transforming growth factor β (TGFβ) family is expressed in the tail bud region of mouse embryos (Gamer et al., 1999; Nakashima et al., 1999), and inactivation of *Gdf11* leads to caudal-to-rostral shift in the identity of paraxial mesodermal derivatives (McPherron et al., 1999). We therefore examined whether Gdf11 might contribute to the patterning of neural Hox-c expression. A chick *Gdf11* cDNA was isolated and its pattern of expression examined. *Gdf11* was not expressed in chick embryos prior to the 11s stage (Figure 6Ai), but from this stage, high levels of expression were detected in HN/tail bud and in caudal paraxial mesoderm (Figures 6Aii–6Aiv). This expression pattern persisted until HH stage 14 (data not shown).

We first examined whether Gdf11, like FGFs, can induce Hox-c expression in MNs in $N_{rc}$ explants. Aggregates of HEK293 cells transfected with *Gdf11* were conjugated with $N_{rc}$ explants, and Hox-c and Isl1(2) expression assayed after 72 hr. *Gdf11*-transfected HEK293 cells did not induce Hoxc6, Hoxc8, Hoxc9, or Hoxc10 expression in Isl1(2)$^+$ MNs (Figure 6C; data not shown). To determine more quantitatively the effect of this class of Gdf proteins on neural Hox-c expression, we also examined the activity of the closely related Gdf family member, Gdf8 (Gamer et al., 1999; Nakashima et al., 1999; Lee and McPherron, 2001). Exposure of $N_{rc}$ explants to 10–40 ng/ml Gdf8

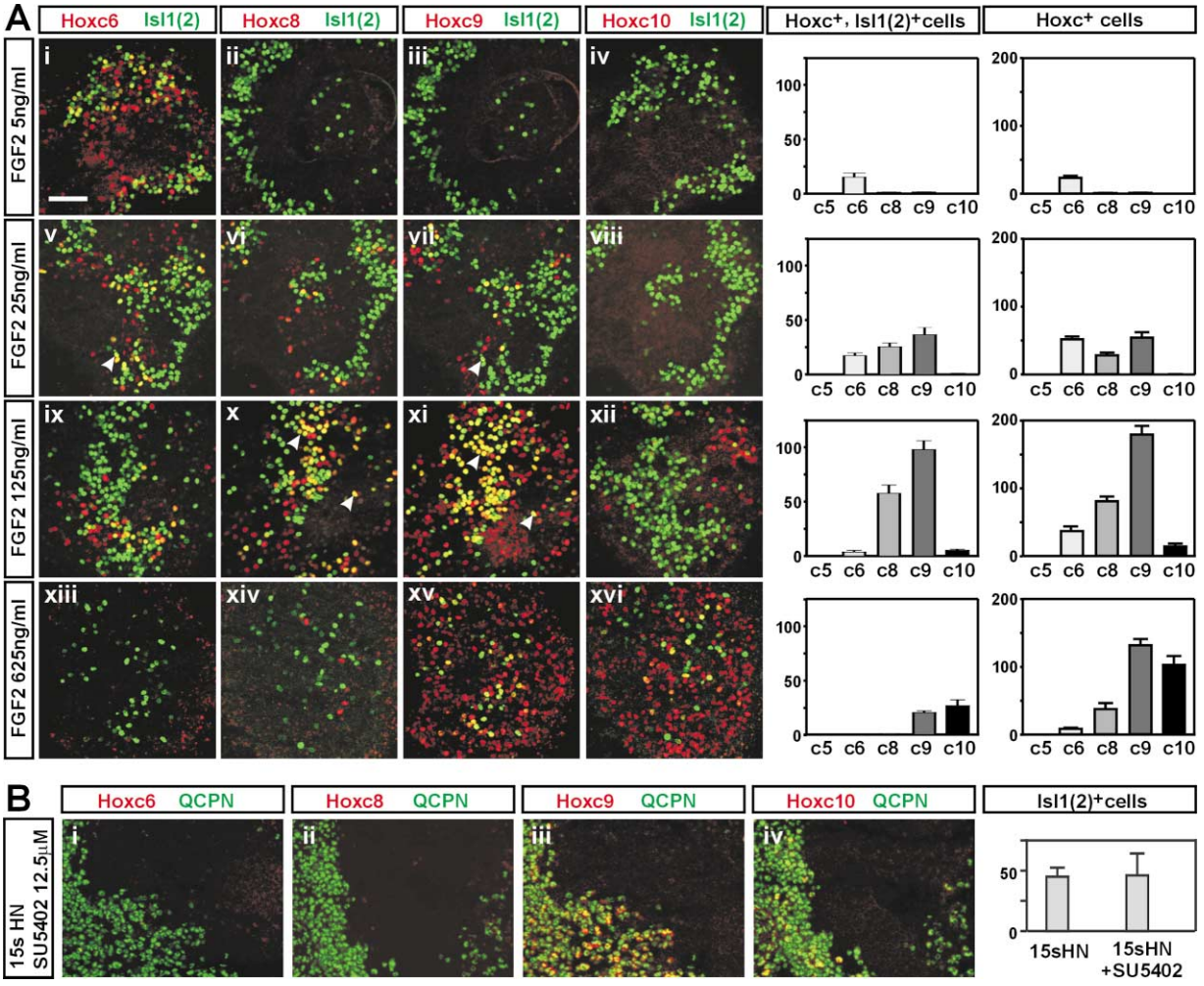


Figure 5. Concentration-Dependent Induction of Hox-c Expression by FGF2

(A) Induction of Hox-c expression by FGF2 in $N_{rc}$ explants. Hox-c proteins are labeled in red and Isl1(2) in green. Panels i and iv, ii and iii, v and vii, vi and viii, x and xi, xiii and xv, and xiv and xvi are the same sections labeled with combinations of Hoxc and Isl1(2) antibodies. Arrowheads in panels v and vii indicate Hoxc6 and Hoxc9 double-labeled MNs, and arrowheads in panels x and xi indicate Hoxc8 and Hoxc9 double-labeled MNs. Hoxc5 expression was not induced.

(B) Addition of SU5402 (12.5 μM) blocks induction of Hox-c proteins in $N_{rc}$ explants by 15s HN. The total number of Isl1(2)$^+$ cells was not affected.

Scale bar: 50 μm.

induced virtually no Hoxc6$^+$, Hoxc8$^+$, Hoxc9$^+$, or Hoxc10$^+$ MNs (Figures 6D and 6E). The number of MNs in $N_{rc}$ explants was reduced in the presence of Gdf8 (Table 1), which may reflect an inhibitory influence on cell proliferation (Kalyani et al., 1998; Lee and McPherron, 2001). Exposure of cells to Gdf8 at these concentrations did not alter the D-V positional character of neural cells (data not shown). Thus, Gdf11 and Gdf8 appear to have little intrinsic Hox-c-inducing activity.

We next examined whether Gdf11/8 modulates the Hox-c patterning activity of FGFs. Exposure of $N_{rc}$ explants to 25 ng/ml FGF2 alone induced Hoxc6$^+$, Hoxc8$^+$, and Hoxc9$^+$, but no Hoxc10$^+$ MNs (Figures 6B and 6I). $N_{rc}$ explants conjugated with *Gdf11*-transfected HEK293 cells and exposed to 25 ng/ml FGF2 exhibited a 4-fold reduction in the number of Hoxc6$^+$ cells, and an ~2-fold increase in the number of Hoxc9$^+$ cells (Figure 6F). Similarly, when $N_{rc}$ explants were exposed jointly to 10 ng/ml Gdf8 and 25 ng/ml FGF2, a 4-fold reduction in Hoxc6$^+$ MN number and a 3-fold increase in Hoxc9$^+$ MN number were observed (Figures 6G and 6J). Joint addition of 40 ng/ml Gdf8 and 25 ng/ml FGF2 virtually abolished expression of Hoxc6 in MNs, increased the number of Hoxc9$^+$ MNs 2-fold, and induced a few Hoxc10$^+$ MNs (Figures 6H and 6K). Together, these results provide evidence that Gdf11 enhances the ability of FGFs to induce a caudal Hox-c profile, thus promoting the differentiation of MNs with a more caudal positional identity.

### A Role for Caudal Mesoderm in Refining Hox-c Expression

Thoracic level neural explants isolated from 14s embryos and grown in vitro aberrantly express Hoxc6 (Figure 2B), raising the possibility that tissues surrounding the neural tube normally have a role in limiting the poste-

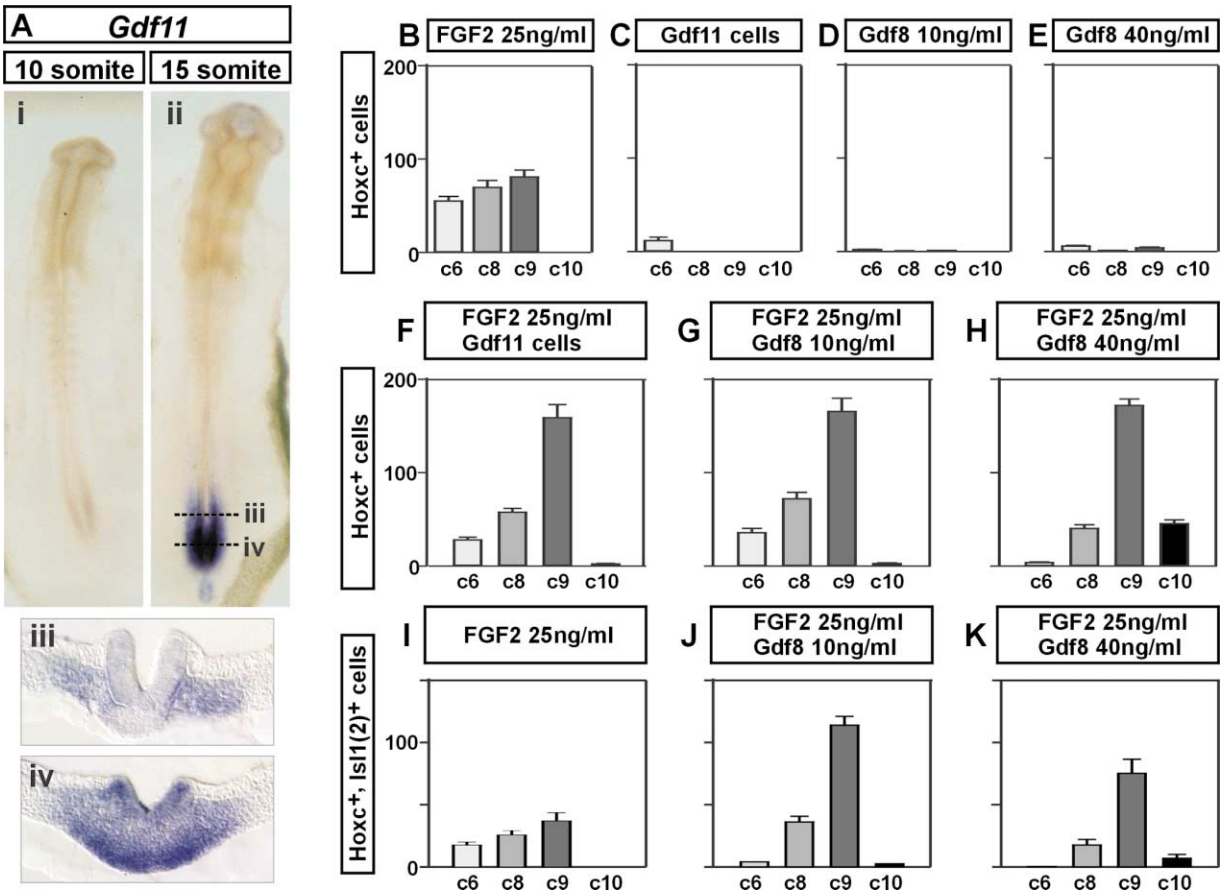


Figure 6. Regulation of Hox-c Expression by Gdfs

(A) Expression of *Gdf11* in chick embryos. (i) *Gdf11* is not detectable in embryos younger than 10s. (ii)–(iv) In older embryos, *Gdf11* is expressed by HN and caudal paraxial mesoderm. A low level of expression is detected in caudal neural plate. Dotted lines in (ii) indicate the levels of cross-sections shown in (iii) and (iv).

(B–K) Quantitation of Hox-c$^+$ cells in $N_{rc}$ explants cultured in the presence of FGF2 and Gdfs.

rior extent of Hoxc6 expression. Since the paraxial mesoderm has been implicated in patterning the neural tube (Ensini et al., 1998; Grapin-Botton et al., 1997; Itasaki et al., 1996), we tested if signals from axial or paraxial mesoderm refine the caudal pattern of neural Hox-c expression. Rostral thoracic level neural tissue from 14s chick embryos ($N_{rt}$ explants, Figures 2B and 2C) was conjugated with 14s quail caudal thoracic level paraxial mesoderm and/or notochord. $N_{rt}$ explants conjugated with either paraxial mesoderm or notochord showed only a small reduction in the number of Hoxc6$^+$ cells, and a small increase in the number of Hoxc9$^+$ cells (data not shown). In contrast, $N_{rt}$ explants conjugated with both paraxial mesoderm and notochord led to an almost complete loss of Hoxc6$^+$ cells, and to an ~2-fold increase in the number of Hoxc9$^+$ cells (Supplemental Figure S4 on *Neuron* website). These studies suggest that the combined actions of signals from thoracic level paraxial mesoderm and notochord repress Hoxc6 and enhance Hoxc9 expression in the thoracic neural tube.

Since *Fgf8* is expressed by posterior notochord and *Gdf11* by posterior paraxial mesoderm at levels flanking thoracic neural tube, we tested if these two factors account for the influence of mesodermal tissues on the pattern of Hox-c expression in the thoracic neural tube. Addition of FGF2 (5 ng/ml) or Gdf8 (5 ng/ml) alone to $N_{rt}$ explants resulted in a small reduction in the number of Hoxc6$^+$ cells and a small increase in the number of Hoxc9$^+$ cells (data not shown). The joint addition of FGF2 (5 ng/ml) and Gdf8 (5 ng/ml) reduced the number of Hoxc6$^+$ cells by >70% and increased the number of Hoxc9$^+$ cells ~1.7-fold (Supplemental Figure S4 on *Neuron* website). Many of the resulting Hox-c$^+$ cells were MNs (data not shown). Thus, at thoracic levels, FGFs and Gdf11 expressed by notochord and posterior paraxial mesoderm, respectively, can act together to refine the profile of Hox-c expression established by signals from HN.

### Retinoid Signaling from Rostral Paraxial Mesoderm Imposes an Anterior Profile of Neural Hox-c Expression

Signals from HN alone are not sufficient to impose a complete rostral profile of Hox-c expression since cervical level neural explants grown in the presence of either HN or FGFs fail to express Hoxc5. We therefore examined the source and nature of signals that confer the profile of Hox-c expression characteristic of the cervical level neural tube.

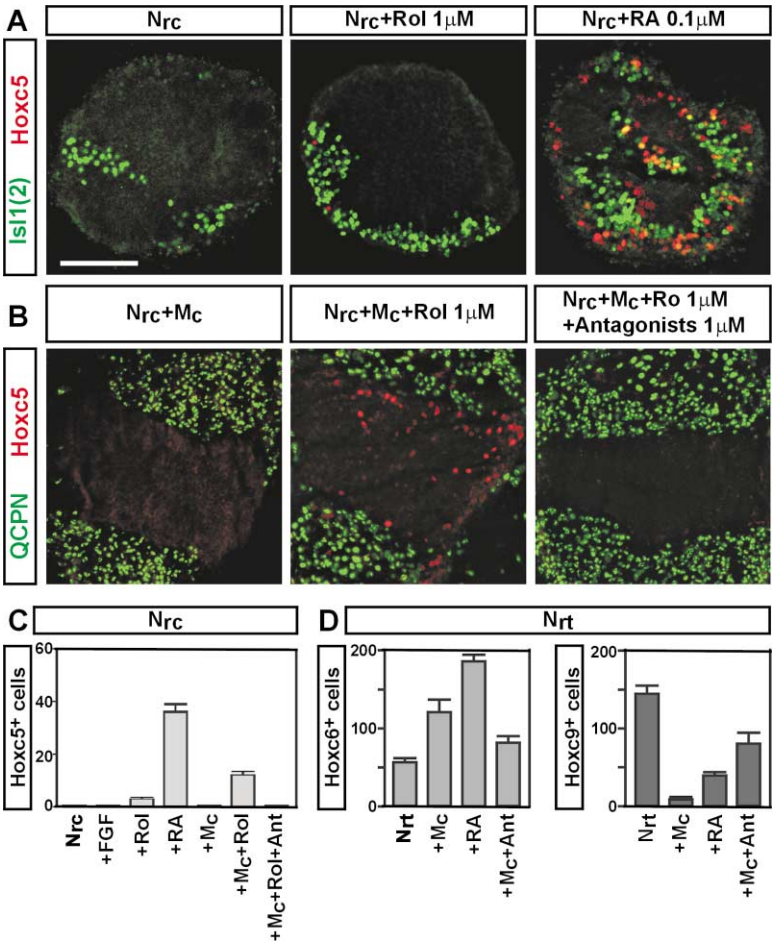


Figure 7. Regulation of Hox-c Expression by Cervical Level Paraxial Mesoderm and Retinoids

(A) $N_{rc}$ explants cultured alone do not express Hoxc5. Addition of retinoic acid (0.1 μM) induces Hoxc5 expression. Many Hoxc5$^+$ cells are MNs, as revealed by Isl1(2) expression. Addition of retinol (1 μM) induces few Hoxc5$^+$ cells.

(B) Cervical level mesoderm ($M_c$) alone does not induce Hoxc5 in $N_{rc}$ explants. In the presence of 1 μM retinol, induction of Hoxc5 is observed. The induction of Hoxc5 is blocked by RAR/RXR antagonists.

(C) Induction of Hoxc5$^+$ cells in $N_{rc}$ explants by retinoids.

(D) Cervical level paraxial mesoderm and retinoids increase the number of Hoxc6$^+$ cells and decrease the number of Hoxc9$^+$ cells in $N_{rt}$ explants.

Scale bar: 50 μm.

To address this issue, $N_{rc}$ explants were grown together with mesodermal tissue isolated from quail embryos, or with candidate-inducing factors. Cervical level paraxial mesoderm expresses a high level of the retinoic acid (RA) synthesizing enzyme retinaldehyde dehydrogenase-2 (RALDH-2) (Berggren et al., 1999; Niederreither et al., 1997; Supplemental Figure S2B), and is a source of retinoid signals that influence the pattern of *Hox-b* expression in the hindbrain (Gould et al., 1998). We tested the involvement of retinoid signaling in the control of Hoxc5 expression by growing $N_{rc}$ explants in the presence of cervical paraxial mesoderm and 1 μM retinol, a precursor of RA that permits efficient RA synthesis by paraxial mesoderm. $N_{rc}$-paraxial mesodermal conjugates grown for 72 hr contained many Hoxc5$^+$ neural cells, whereas cells in $N_{rc}$ explants grown alone, or in 1 μM retinol, contained few if any Hox5$^+$ cells (Figures 7A–7C). $N_{rc}$ explants grown in the presence of 0.1 μM RA without paraxial mesoderm or retinol also generated many Hoxc5$^+$ cells (Figures 7A and 7C). Of these Hoxc5$^+$ cells, ~40% were Isl1(2)$^+$ MNs (Figure 7A, data not shown). Exposure of 5s $N_{rc}$ explants to 0.1 μM RA did not induce expression of Hoxc6, Hoxc8, Hoxc9, or Hoxc10 in MNs or other cells (data not shown), providing evidence that retinoids do not substitute for FGFs in the induction of these Hox-c proteins. Exposure of $N_{rc}$ explants to retinoids produced a significant increase in total MN number (Table 1), consistent with the mitogenic effect of retinoids on neural progenitors (Sockanathan and Jessell, 1998). These results provide evidence that retinoids synthesized by the paraxial mesoderm induce expression of Hoxc5 in MNs. To test whether retinoid signals from paraxial mesoderm are required for the neural expression of Hoxc5, $N_{rc}$ explants were conjugated with cervical level paraxial mesoderm in the presence of 1 μM retinol and the retinoic acid receptor (RAR) and retinoid X receptor (RXR) antagonists LG100815 (1 μM), and LG100849 (1 μM) (Sockanathan and Jessell, 1998). No neural expression of Hoxc5 was detected under these conditions (Figure 7B). These findings provide evidence that retinoid signals from cervical level paraxial mesoderm are required for the expression of Hoxc5 in MNs.

We next examined whether retinoid signaling from cervical level paraxial mesoderm also modifies the profile of Hoxc6, Hoxc8, and Hoxc9 expression—Hox-c proteins that are induced in MNs by FGF-mediated signals from HN. We exposed explants isolated from prospective thoracic levels of the neural tube ($N_{rt}$ explants) to cervical level paraxial mesoderm or to retinoids. Conjugating 14s $N_{rt}$ tissue with 14s cervical level paraxial mesoderm led to an ~2-fold increase in Hoxc6$^+$ cells and to a 3-fold decrease in Hoxc8$^+$ and a 6-fold decrease in Hoxc9$^+$ cells (Figure 7D, data not shown). 14s $N_{rt}$ explants grown in the presence of 0.1 μM RA exhibited an ~2-fold increase in Hoxc6$^+$, Isl1(2)$^+$ MNs,

and an ~3-fold decrease in Hoxc8$^+$, Isl1(2)$^+$ and Hoxc9$^+$, Isl1(2)$^+$ MNs (Figure 7D, data not shown). The ability of cervical level paraxial mesoderm to increase Hoxc6 and decrease Hoxc8 and Hoxc9 expression was partially blocked by addition of RA receptor antagonists (Figure 7D, data not shown). Thus, retinoid signaling from cervical level paraxial mesoderm appears to refine the pattern of Hox-c expression induced in MNs by FGF signals from HN. These findings, together with the RA-mediated induction of Hoxc5, indicate that retinoid signaling from cervical level paraxial mesoderm is involved in conferring a complete rostral profile of Hox-c expression to MNs in the cervical spinal cord.

### Patterning of Neural Hox-c Expression by FGF Signaling In Vivo

We next determined whether FGF signaling also regulates neural Hox-c expression in vivo. We misexpressed a mutated form of the FGF receptor 1 (FGFR1*) which activates FGF signal transduction in a ligand-independent manner (Hart et al., 2000). We reasoned that cells that express FGFR1* should behave as if they have been exposed to elevated levels of FGF signaling, and thus will undergo a rostral-to-caudal shift in their profile of Hox-c expression. We selected an activated FGF receptor 1 for these studies since the inhibitory activity of SU5402 on Hox-c expression implicates this FGF receptor subtype in neural patterning. FGFR1* was expressed unilaterally at brachial and cervical levels of the neural tube by electroporation into 9s–12s embryos, followed by analysis of neural Hox-c pattern at HH stages 20–21 and 24–25.

Expression of FGFR1* at brachial levels resulted in ectopic rostral expression of Hoxc9 and Hoxc10 in ventral regions of the spinal cord, coincident with local sites of ectopic FGFR1* expression (Figures 8C, 8D, 8G, and 8H). Some, but not all, ectopic Hoxc9$^+$ or Hoxc10$^+$ cells coexpressed MN markers. In contrast, FGFR1* expression suppressed the expression of Hoxc6 and to a lesser extent Hoxc8 from brachial level MNs (Figures 8E, 8E′, 8F, and 8F′). The ectopic rostral expression of Hoxc9 and Hoxc10 elicited by FGFR1* expression was also observed at more dorsal levels of the spinal cord (Figures 8C, 8D, 8G, and 8H). In some experiments, ectopic rostral expression of Hoxc9 and Hoxc10 could also be detected at cervical levels of the spinal cord (data not shown). Ectopic expression of an analogous wild-type FGFR1 had no effect on Hox-c pattern (Figures 8I–8L′; data not shown). Together, these results support the idea that FGF signaling regulates neural Hox-c pattern in vivo.

## Discussion

Hox proteins control many features of vertebrate CNS development. In this study, we have examined the signals that establish the R-C pattern of Hox-c expression in MNs in the developing spinal cord. Our findings indicate that signals derived from HN initiate the R-C pattern of neuronal Hox-c expression, but the final pattern of Hox-c expression appears to depend on additional signals provided by the paraxial mesoderm (Figure 9). HN signals appear to be mediated in large part by FGFs, and the graded signaling activity of FGFs appears to specify many aspects of the position-dependent profile of neuronal Hox-c expression (Figure 9B). However, the complete profile of neuronal Hox-c expression at cervical levels of the spinal cord requires retinoid signaling from cervical level paraxial mesoderm. The profile of Hox-c expression at caudal thoracic and rostral lumbar levels appears to be refined by the activity of a TGFβ family member, Gdf11, expressed selectively at caudal levels in HN and the adjacent paraxial mesoderm (Figure 9). We discuss these findings in the context of the contributions of patterning signals from axial and paraxial mesoderm in specifying the positional identity of MNs.

### Hensen's Node Signaling and the Initiation of Hox-c Expression

Signals from prospective axial mesodermal tissues, HN and the primitive streak, appear to induce Hox-c expression in MNs in a position-appropriate manner. Thus, HN tissue from embryos of progressively older stages induces a profile of Hox-c expression characteristic of progressively more caudal levels of the spinal cord. These findings extend previous observations that HN has age-dependent activities in specifying the fate of cells at midbrain and hindbrain levels of the neural axis (Kintner and Dodd, 1991; Storey et al., 1992). With the exception of Hoxc5, Hox-c inductive activity is largely confined to HN and the newly formed notochord.

The profile of Hox-c inductive activity exhibited by HN coincides well with the expression pattern of *FGF* genes, notably *Fgf8*. FGFs act in vitro in a graded manner, with higher concentrations of FGFs inducing a progressively more caudal profile of neural Hox-c expression. Similarly, activation of FGF receptor signaling in vivo induces a rostral-to-caudal shift in the profile of Hox-c expression. We note that in these in vivo studies, not all ectopic Hoxc9$^+$ and Hoxc10$^+$ cells located in the ventral spinal cord expressed MN markers, which may indicate additional actions of high level FGF signaling on MN differentiation. Nevertheless, together these in vitro and in vivo findings indicate that graded FGF signals derived from HN are likely to initiate the neural pattern of Hox-c expression. Such graded signaling could be achieved by a stage-dependent increase in the level of FGF signaling from HN since the level of *Fgf8* expression in HN appears to increase in older embryos. Alternatively, since neural cells fated to give rise to progressively more caudal regions of the spinal cord are positioned close to HN for progressively longer periods, they may be exposed to the same level of FGF signaling as cells destined to populate more rostral regions of the spinal cord, but for a longer period. Recent studies have provided evidence that FGF signaling within HN promotes the proliferation of prospective neural cells, maintaining a progenitor cell population throughout the period of spinal cord elongation (Mathis et al., 2001). Thus, FGF signaling within HN may coordinate the proliferation and R-C specification of spinal progenitor cells.

The onset of expression of the Hox-c proteins by spinal MNs occurs after neurons have left the cell cycle, yet our findings indicate that patterned Hox-c expression is specified at the time of neural plate formation. How is the early specification of positional identity linked to the

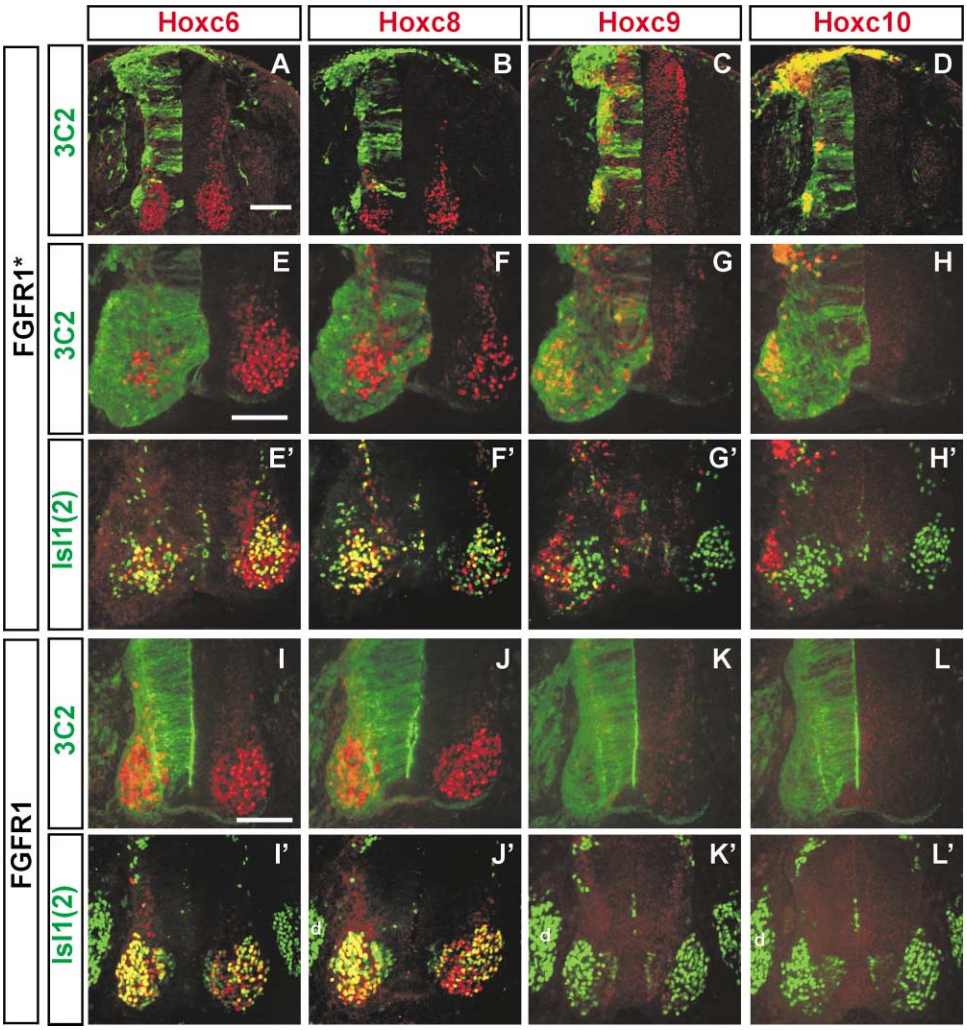


Figure 8. Repatterning of Hox-c Expression by Constitutively Activated FGFR1 In Vivo

(A–D) Patterns of ectopic Hoxc9 and Hoxc10 expression at brachial spinal cord 48 hr after electroporation of constitutively activated FGFR1 (FGFR1*) (HH stage 20–21).

(E–H and E'–H') 72 hr after electroporation of FGFR1* (HH stage 24–25), the induction of ectopic Hoxc9 and Hoxc10 and the repression of Hoxc6 and Hoxc8 are evident in domains of retroviral expression at brachial levels. Some but not all ectopic Hoxc9$^{+}$ and Hoxc10$^{+}$ cells are MNs, as assessed by Isl1(2) expression.

(I–L and I'–L') No repatterning of Hox-c expression is evident 72 hr after electroporation of wild-type FGFR1. "d" indicates dorsal root ganglia. Scale bars: 100 μm.

expression of Hox-c proteins in MNs? In *Xenopus*, the FGF-dependent regulation of *Hox* gene expression in mesodermal and neural cells involves *Cdx* genes (Isaacs et al., 1998; Pownall et al., 1996). Different members of *Cdx* gene family appear to be expressed at different R-C levels during early stages of chick neural development (Marom et al., 1997). Thus, *Cdx* genes are plausible mediators of FGF signaling in the regulation of Hox-c expression within MNs.

### Signals from Paraxial Mesoderm Refine the Initial Pattern of Neural Hox-c Expression

Many aspects of the R-C pattern of Hox-c expression in spinal MNs can be accounted for by the action of FGFs provided by HN. But three observations indicate that additional signals are required to achieve the profile of Hox-c expression evident at cervical and lumbar levels. First, neither HN nor FGFs induce the neural expression of Hoxc5, a Hox-c protein that delineates cervical levels of the spinal cord. Second, segments of the thoracic neural tube isolated after the influence of HN-derived signals exhibit ectopic caudal expression of Hoxc6, suggesting that the normal caudal limit of Hoxc6 expression is defined by signals that act later than those provided by HN. Third, Hoxc10 expression is induced only at very high FGF concentrations, suggesting that the acquisition of a caudal Hox-c profile requires additional signals.

One source of these additional signals appears to be the paraxial mesoderm. Paraxial mesodermal signals refine the R-C pattern of neuronal Hox-c expression initiated by FGF signals from the primitive streak and HN. Rostral paraxial mesoderm expresses high levels

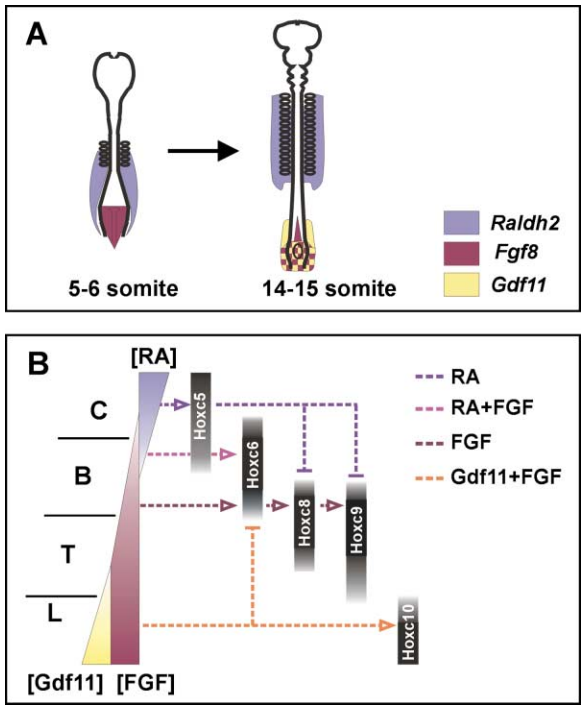


Figure 9. Convergent Signals Establish the Rostrocaudal Pattern of Hox-c Expression in Developing Spinal Cord

(A) Expression domains of *Raldh2*, *Fgf8*, and *Gdf11* in 5s–6s and 14s–15s embryos.

(B) Summary of combinatorial actions of FGFs, RA, and Gdf11 in specifying the R-C Hox-c profile in developing spinal cord. Low concentrations of FGF induce Hoxc6 and higher concentrations induce Hoxc8 and Hoxc9. In the cervical spinal cord, RA induces Hoxc5. In rostral brachial levels, RA also upregulates Hoxc6 and inhibits Hoxc8 and Hoxc9. At more caudal levels of the spinal cord, Gdf11 appears to act with FGFs to induce Hoxc10 and inhibit Hoxc6. The restricted distribution of these factors along the R-C axis of the embryo appears to establish the patterned expression of Hox-c proteins in MNs.

of retinoid signaling activity (Maden et al., 1998), and retinoids rather than FGFs induce the expression of Hoxc5 at cervical levels. Retinoid signaling also refines the expression pattern of Hox-c proteins whose expression is initiated by FGF signals from HN. Retinoid signaling from rostral paraxial mesoderm therefore appears necessary to establish a cervical profile of Hox-c expression in MNs.

Previous studies have implicated early retinoid signaling in establishing the generic character of the spinal cord (Muhr et al., 1999), and later retinoid signaling in defining the pattern of *Hox* gene expression in the developing hindbrain (Gavalas and Krumlauf, 2000; Niederreither et al., 2000). Both activities reveal that retinoids can exert a caudalizing influence on neural tissue. Our studies invoke a late role for retinoids in establishing regional identity within the spinal cord itself. Thus, paraxial mesodermal sources of retinoids appear to act at sequential developmental stages to impose different R-C positional values to cells in the spinal cord and hindbrain. In addition, in the context of spinal cord development, they indicate that retinoids impose a rostral rather than caudal positional character, and thus, inferences about rostralizing or caudalizing influences of retinoids depend on the specific domain of the neural axis under study.

Do retinoids have an equivalent role in R-C patterning at more caudal levels of the spinal cord? Paraxial mesoderm at prospective thoracic levels expresses *Raldh2*, but its onset of expression occurs at a later stage and its expression level is lower than that in the cervical level mesoderm (Berggren et al., 1999; Niederreither et al., 1997). By the time of its caudal expression, the initial specification of neural Hox-c expression has been established, and there has been a marked decrease in the competence of thoracic neural tissue to respond to retinoid signaling with changes in Hox-c expression (unpublished observations). At these more caudal levels, HN and the paraxial mesoderm selectively expresses Gdf11, a member of the TGFβ family. Gdf11 alone appears to have little Hox-c-inducing ability, but in conjunction with FGF signaling, markedly alters the profile of Hox-c expression. The prominent expression of Hoxc9 and Hoxc10 normally observed at caudal thoracic and rostral lumbar levels of the spinal cord may therefore be achieved through the joint exposure of neural cells to FGFs and Gdf11. A role for Gdf11 in establishing the lumbar character of the paraxial mesoderm has emerged from studies of *Gdf11* mouse mutants (McPherron et al., 1999). Our studies reveal a role for Gdf11 in patterning the neural tube, independent of its actions on mesodermal tissues, and raise the possibility that the actions of Gdf11 on caudal paraxial mesoderm may also reflect the modulation of FGF signaling.

The involvement of HN signaling in establishing the spinal Hox-c expression profile may help to explain the results of in vivo grafting studies that examined the source of signals that define the pattern of *Hoxd10* expression at the lumbar spinal cord. Here, signals from paraxial mesoderm are not sufficient to explain the neural pattern of *Hoxd10* expression (Lance-Jones et al., 2001). Our studies suggest that FGF and Gdf11 signals from HN may also control *Hox-d* expression at lumbar levels, in a manner similar to their role in patterning *Hox-c* expression.

### Mesodermal Signaling and the Specification of MN Subtype Identity

Our studies also provide additional insights into the contributions of mesodermal signals to the specification of MN subtype identity. Signals from HN and the notochord, notably Shh and BMP antagonists, have been implicated in the D-V patterning events that establish the generic identity of MNs (Jessell, 2000; Liem et al., 2000; McMahon et al., 1998). Neither Shh nor BMP antagonists, however, appear to have a role in spinal MN subtype specification (Briscoe and Ericson, 2001). Instead, FGFs—a class of signals expressed by HN and transiently by the notochord—appear to be involved in controlling the subtype identity of spinal MNs. These results are consistent with the view that the specification of neuronal identity along the D-V and R-C axes of the spinal cord is controlled through largely independent signaling pathways. FGFs, retinoids, and Gdfs appear to alter progenitor cell proliferation in addition to regulating the Hox-c expression profile (Mathis et al., 2001; Socka-

nathan and Jessell, 1998; this study). As a consequence, MN number is altered by manipulations that influence neural Hox-c expression. Nevertheless, the change in neuronal Hox-c status appears to be achieved independently of controls on MN number.

Our studies have emphasized the key role of signals from the primitive streak and HN in establishing the R-C pattern of Hox-c expression. Other aspects of the R-C identity of spinal MNs may, however, be controlled by signals from the paraxial mesoderm. Specification of the LMC columnar subdivision of MNs is controlled by signals from limb level paraxial mesoderm that operate soon after neural tube closure (Ensini et al., 1998). Neither the patterns of *Gdf11* nor retinoid expression at these developmental stages readily explain this limb level-restricted signaling activity of the paraxial mesoderm. It is likely, therefore, that the paraxial mesoderm provides an additional signal devoted to the allocation of MN columnar identity. Are other features of MN subtype identity also controlled by mesodermal signals? Aspects of the pool identity of MNs within the LMC, defined by the projection pattern of motor axons and by expression of *ETS* genes, can be altered by changing the positional relationship between limb levels of the neural tube and adjacent paraxial mesoderm (Lin et al., 1998; Matise and Lance-Jones, 1996). Since in these studies grafted regions of the neural tube are manipulated at early developmental stages, it is unclear whether the establishment of motor pool identity depends solely on signals from paraxial mesoderm, or can be influenced by earlier signals from HN. Nevertheless, certain motor pool characteristics, notably *ETS* gene expression, are dependent on signals encountered by motor axons as they enter the lateral plate mesoderm at limb levels (Lin et al., 1998). Thus, three major mesodermal cell types, axial mesoderm, paraxial mesoderm, and lateral plate mesoderm, regulate distinct features of the R-C identity of spinal MNs, presumably through the provision of diverse extrinsic signals.

## Experimental Procedures

### Generation of Anti-Hox-c Antibodies

cDNAs corresponding to the N-terminal region of Hox-c proteins were subcloned into pGex5X vectors. Fusion proteins were purified and injected into mice, rabbits, or guinea pigs.

### Cloning of Chick *Gdf11*

First strand cDNA was prepared with total RNA isolated from the posterior region of HH stage 13–14 embryos (Hamburger and Hamilton, 1951). A ~730 bp cDNA corresponding to amino acids 132–383 (missing aa 210–217) of human *GDF11* was generated by PCR using GARGARGAYGARTAYCA and CRTTRAARTANAGCATRTT primers. This clone shows 99% sequence conservation with human and mouse GDF11. (R = A or G, Y = C or T, N = A or T or C or G.)

### Neural Explant Culture

Neural explants were isolated from different regions and stages of chick embryos. Their fates were determined by DiI labeling (see Supplemental Data at http://www.neuron.org/cgi/content/full/32/6/997/DC1).

HN tissue (all three germ layers) including rostral primitive streak was isolated from 5s–6s and 10s–11s quail embryos. Tail bud tissues (all three germ layers) were isolated from 14s–15s and 19s–20s quail embryos. Cervical level mesoderm tissue was isolated from regions anterior to HN in 5s–6s quail embryos (for conjugation with $N_{rc}$), or from regions posterior to the somites in 14s–15s quail embryos (for conjugates with $N_{rt}$). Thoracic level mesoderm and notochord tissues were isolated from regions anterior to HN (tail bud) in 14s–15s quail embryos. Tissues were cultured in serum-free medium in a collagen gel matrix (Liu and Jessell, 1998).

### In Ovo Electroporation

RIS plasmids encoding replication in competent retroviruses that contain constitutively active FGFR1 (FGFR1*, RIS174HA) and control wild-type FGFR1 (RIS172HA) genes were generated using myristylated, cytoplasmic forms of the FGFR1 gene (Hart et al., 2000) into which an HA epitope tag was inserted. DNA (5 μg/μl) was electroporated into the neural tube in ovo using five pulses at 30 V; 50 ms. Embryos were analyzed at 48 hr (HH stage 20–21) or 72 hr (HH stage 24–25). The AMV-3C2 viral gag antibody made by D. Boettiger was obtained from the Developmental Studies Hybridoma Bank.

### Preparation of Secreted Factors

Heparin beads (Sigma) were soaked with 11–100 μg/ml FGF8b (R&D system) (Storey et al., 1998) and conjugated with neural explants. FGF2 (Life Technologies), SU5402 (Calbiochem), Gdf8 (provided by S-J Lee), all-trans retinoic acid (Sigma), all-trans retinol (Sigma), LG100815, and LG100849 (Ligand Pharmaceuticals, provided by S. Sockanathan) were added at concentrations indicated.

pCI-neo (Promega) plasmids containing human *GDF11* and IRES-eGFP, or *BMP2* pro-region with *GDF11* mature region and IRES-eGFP, were transfected into HEK293 cells, selected with 1.5 mg/ml G418, and FACS sorted for GFP expression. Sorted cells were then transfected with an SPC1 expression plasmid (Constam and Robertson, 1999) to enhance processing to the mature GDF11 protein. After 24 hr, aggregates of 500–1000 cells were prepared in 20 μl hanging drops and conjugated with neural explants.

### Immmunohistochemistry and Cell Counting

Explant tissues in collagen matrix were fixed and prepared for cryosection (Liu and Jessell, 1998). Details of antisera and immunohistochemical procedures are available as Supplemental Data on *Neuron* website.

### Acknowledgments

We are grateful to S. Morton for help in generating antibodies, I. Schieren for FACS expertise, K. MacArthur for help in preparing the manuscript, I. Messina for technical assistance, M. Webster and D. Donoghue for the FGFR1 constructs, C. Tabin for *Hox-c* cDNAs, P. Gruss for *Hoxc8* and *Hoxc9* cDNAs, S.-J. Lee for *GDF11* cDNA and Gdf8 protein, A. Streit for *Fgf8* cDNA, and E. Robertson for the *SPC1* plasmid. We thank M. Ensini, B. Han, S. Sockanathan, A. Streit, and T. Tsuchida for advice; and S. Sockanathan, J. Dasen, and S. Zeitlin for comments on the manuscript. J.-P. L. is a recipient of a Burroughs Wellcome Fund Career Award in the Biomedical Sciences. E.L. was supported by Basil O'Connor Scholar Grant #5-FY99-855 from the March of Dimes Birth Defects Foundation and the HHMI Research Resources Program for Medical Schools. T.M.J. was supported by grants from NINDS and Project ALS, and is an HHMI Investigator.

Received August 14, 2001; revised November 15, 2001.

### References

Bell, E., Wingate, R.J., and Lumsden, A. (1999). Homeotic transformation of rhombomere identity after localized Hoxb1 misexpression. Science *284*, 2168–2171.

Belting, H.G., Shashikant, C.S., and Ruddle, F.H. (1998). Multiple phases of expression and regulation of mouse Hoxc8 during early embryogenesis. J. Exp. Zool. *282*, 196–222.

Berggren, K., McCaffery, P., Drager, U., and Forehand, C.J. (1999). Differential distribution of retinoic acid synthesis in the chicken embryo as determined by immunolocalization of the retinoic acid synthetic enzyme, RALDH-2. Dev. Biol. *210*, 288–304.

Briscoe, J., and Ericson, J. (2001). Specification of neuronal fates in the ventral neural tube. Curr. Opin. Neurobiol. *11*, 43–49.

Carpenter, E.M., Goddard, J.M., Davis, A.P., Nguyen, T.P., and Capecchi, M.R. (1997). Targeted disruption of Hoxd-10 affects mouse hindlimb development. Development *124*, 4505–4514.

Constam, D.B., and Robertson, E.J. (1999). Regulation of bone morphogenetic protein activity by pro domains and proprotein convertases. J. Cell Biol. *144*, 139–149.

Crossley, P.H., and Martin, G.R. (1995). The mouse Fgf8 gene encodes a family of polypeptides and is expressed in regions that direct outgrowth and patterning in the developing embryo. Development *121*, 439–451.

de la Cruz, C.C., Der-Avakian, A., Spyropoulos, D.D., Tieu, D.D., and Carpenter, E.M. (1999). Targeted disruption of Hoxd9 and Hoxd10 alters locomotor behavior, vertebral identity, and peripheral nervous system development. Dev. Biol. *216*, 595–610.

Ensini, M., Tsuchida, T.N., Belting, H.G., and Jessell, T.M. (1998). The control of R-C pattern in the developing spinal cord: specification of MN subtype identity is initiated by signals from paraxial mesoderm. Development *125*, 969–982.

Ericson, J., Morton, S., Kawakami, A., Roelink, H., and Jessell, T.M. (1996). Two critical periods of Sonic Hedgehog signaling required for the specification of MN identity. Cell *87*, 661–673.

Forehand, C.J., Ezerman, E.B., Rubin, E., and Glover, J.C. (1994). Segmental patterning of rat and chicken sympathetic preganglionic neurons: correlation between soma position and axon projection pathway. J. Neurosci. *14*, 231–241.

Gamer, L.W., Wolfman, N.M., Celeste, A.J., Hattersley, G., Hewick, R., and Rosen, V. (1999). A novel BMP expressed in developing mouse limb, spinal cord, and tail bud is a potent mesoderm inducer in Xenopus embryos. Dev. Biol. *208*, 222–232.

Gavalas, A., and Krumlauf, R. (2000). Retinoid signalling and hindbrain patterning. Curr. Opin. Genet. Dev. *10*, 380–386.

Gavalas, A., Davenne, M., Lumsden, A., Chambon, P., and Rijli, F.M. (1997). Role of Hoxa-2 in axon pathfinding and rostral hindbrain patterning. Development *124*, 3693–3702.

Gould, A., Itasaki, N., and Krumlauf, R. (1998). Initiation of rhombomeric Hoxb4 expression requires induction by somites and a retinoid pathway. Neuron *21*, 39–51.

Grapin-Botton, A., Bonnin, M.A., and Le Douarin, N.M. (1997). Hox gene induction in the neural tube depends on three parameters: competence, signal supply and paralogue group. Development *124*, 849–859.

Hamburger, V., and Hamilton, H.L. (1951). A series of normal stages in the development of the chick embryo. J. Morphol. *88*, 49–92.

Hart, K.C., Robertson, S.C., Kanemitsu, M.Y., Meyer, A.N., Tynan, J.A., and Donoghue, D.J. (2000). Transformation and Stat activation by derivatives of FGFR1, FGFR3, and FGFR4. Oncogene *19*, 3309–3320.

Hollyday, M. (1980a). Organization of motor pools in the chick lumbar lateral motor column. J. Comp. Neurol. *194*, 143–170.

Hollyday, M. (1980b). Motoneuron histogenesis and the development of limb innervation. Curr. Top. Dev. Biol. *15*, 181–215.

Hollyday, M., and Hamburger, V. (1977). An autoradiographic study of the formation of the lateral motor column in the chick embryo. Brain Res. *132*, 197–208.

Isaacs, H.V., Pownall, M.E., and Slack, J.M. (1998). Regulation of Hox gene expression and posterior development by the Xenopus caudal homologue Xcad3. EMBO J. *17*, 3413–3427.

Itasaki, N., Sharpe, J., Morrison, A., and Krumlauf, R. (1996). Reprogramming Hox expression in the vertebrate hindbrain: influence of paraxial mesoderm and rhombomere transposition. Neuron *16*, 487–500.

Jessell, T.M. (2000). Neuronal specification in the spinal cord: inductive signals and transcriptional codes. Nat. Rev. Genet. *1*, 20–29.

Jungbluth, S., Bell, E., and Lumsden, A. (1999). Specification of distinct MN identities by the singular activities of individual Hox genes. Development *126*, 2751–2758.

Kalyani, A.J., Piper, D., Mujtaba, T., Lucero, M.T., and Rao, M.S. (1998). Spinal cord neuronal precursors generate multiple neuronal phenotypes in culture. J. Neurosci. *18*, 7856–7868.

Kania, A., Johnson, R.L., and Jessell, T.M. (2000). Coordinate roles for LIM homeobox genes in directing the D-V trajectory of motor axons in the vertebrate limb. Cell *102*, 161–173.

Kintner, C.R., and Dodd, J. (1991). Hensen's node induces neural tissue in Xenopus ectoderm. Implications for the action of the organizer in neural induction. Development *113*, 1495–1505.

Lance-Jones, C., Omelchenko, N., Bailis, A., Lynch, S., and Sharma, K. (2001). *Hoxd10* induction and regionalization in the developing lumbosacral spinal cord. Development *128*, 2252–2268.

Landmesser, L.T. (1978a). The development of motor projection patterns in the chick hind limb. J. Physiol. *284*, 391–414.

Landmesser, L.T. (1978b). The distribution of motoneurones supplying chick hind limb muscles. J. Physiol. *284*, 371–389.

Landmesser, L.T. (2001). The acquisition of motoneuron subtype identity and motor circuit formation. Int. J. Dev. Neurosci. *19*, 175–182.

Laskowski, M.B., and Sanes, J.R. (1987). Topographic mapping of motor pools onto skeletal muscles. J. Neurosci. *7*, 252–260.

Lee, K.J., and Jessell, T.M. (1999). The specification of dorsal cell fates in the vertebrate central nervous system. Annu. Rev. Neurosci. *22*, 261–294.

Lee, S.J., and McPherron, A.C. (2001). Regulation of myostatin activity and muscle growth. Proc. Natl. Acad. Sci. USA *98*, 9306–9311.

Liem, K.F., Jr., Jessell, T.M., and Briscoe, J. (2000). Regulation of the neural patterning activity of sonic hedgehog by secreted BMP inhibitors expressed by notochord and somites. Development *127*, 4855–4866.

Lin, J.H., Saito, T., Anderson, D.J., Lance-Jones, C., Jessell, T.M., and Arber, S. (1998). Functionally related MN pool and muscle sensory afferent subtypes defined by coordinate ETS gene expression. Cell *95*, 393–407.

Liu, J.P., and Jessell, T.M. (1998). A role for rhoB in the delamination of neural crest cells from the dorsal neural tube. Development *125*, 5055–5067.

Lumsden, A., and Krumlauf, R. (1996). Patterning the vertebrate neuraxis. Science *274*, 1109–1115.

Maden, M., Sonneveld, E., van der Saag, P.T., and Gale, E. (1998). The distribution of endogenous retinoic acid in the chick embryo: implications for developmental mechanisms. Development *125*, 4133–4144.

Mahmood, R., Kiefer, P., Guthrie, S., Dickson, C., and Mason, I. (1995a). Multiple roles for FGF-3 during cranial neural development in the chicken. Development *121*, 1399–1410.

Mahmood, R., Bresnick, J., Hornbruch, A., Mahony, C., Morton, N., Colquhoun, K., Martin, P., Lumsden, A., Dickson, C., and Mason, I. (1995b). A role for FGF-8 in the initiation and maintenance of vertebrate limb bud outgrowth. Curr. Biol. *5*, 797–806.

Marom, K., Shapira, E., and Fainsod, A. (1997). The chicken caudal genes establish an anterior-posterior gradient by partially overlapping temporal and spatial patterns of expression. Mech. Dev. *64*, 41–52.

Mathis, L., Kulesa, P.M., and Fraser, S.E. (2001). FGF receptor signalling is required to maintain neural progenitors during Hensen's node progression. Nat. Cell Biol. *3*, 559–566.

Matise, M.P., and Lance-Jones, C. (1996). A critical period for the specification of motor pools in the chick lumbosacral spinal cord. Development *122*, 659–669.

McMahon, J.A., Takada, S., Zimmerman, L.B., Fan, C.M., Harland, R.M., and McMahon, A.P. (1998). Noggin-mediated antagonism of BMP signaling is required for growth and patterning of the neural tube and somite. Genes Dev. *12*, 1438–1452.

McPherron, A.C., Lawler, A.M., and Lee, S.J. (1999). Regulation of anterior/posterior patterning of the axial skeleton by growth/differentiation factor 11. Nat. Genet. *22*, 260–264.

Mohammadi, M., McMahon, G., Sun, L., Tang, C., Hirth, P., Yeh, B.K., Hubbard, S.R., and Schlessinger, J. (1997). Structures of the tyrosine kinase domain of fibroblast growth factor receptor in complex with inhibitors. Science *276*, 955–960.

Muhr, J., Graziano, E., Wilson, S., Jessell, T.M., and Edlund, T. (1999). Convergent inductive signals specify midbrain, hindbrain, and spinal cord identity in gastrula stage chick embryos. Neuron *23*, 689–702.

Nakashima, M., Toyono, T., Akamine, A., and Joyner, A. (1999). Expression of growth/differentiation factor *11*, a new member of the BMP/TGFbeta superfamily during mouse embryogenesis. Mech. Dev. *80*, 185–189.

Niederreither, K., McCaffery, P., Drager, U.C., Chambon, P., and Dolle, P. (1997). Restricted expression and retinoic acid-induced downregulation of the retinaldehyde dehydrogenase type 2 (RALDH-2) gene during mouse development. Mech. Dev. *62*, 67–78.

Niederreither, K., Vermot, J., Schuhbaur, B., Chambon, P., and Dolle, P. (2000). Retinoic acid synthesis and hindbrain patterning in the mouse embryo. Development *127*, 75–85.

Niswander, L., and Martin, G.R. (1992). Fgf-4 expression during gastrulation, myogenesis, limb and tooth development in the mouse. Development *114*, 755–768.

Patten, I., and Placzek, M. (2000). The role of Sonic hedgehog in neural tube patterning. Cell. Mol. Life Sci. *57*, 1695–1708.

Pownall, M.E., Tucker, A.S., Slack, J.M., and Isaacs, H.V. (1996). eFGF, Xcad3 and Hox genes form a molecular pathway that establishes the anteroposterior axis in Xenopus. Development *122*, 3881–3892.

Riese, J., Zeller, R., and Dono, R. (1995). Nucleo-cytoplasmic translocation and secretion of fibroblast growth factor-2 during avian gastrulation. Mech. Dev. *49*, 13–22.

Roghani, M., Mansukhani, A., Dell'Era, P., Bellosta, P., Basilico, C., Rifkin, D.B., and Moscatelli, D. (1994). Heparin increases the affinity of basic fibroblast growth factor for its receptor but is not required for binding. J. Biol. Chem. *269*, 3976–3984.

Schoenwolf, G.C. (1992). Morphological and mapping studies of the paranodal and postnodal levels of the neural plate during chick neurulation. Anat. Rec. *233*, 281–290.

Sharma, K., Sheng, H.Z., Lettieri, K., Li, H., Karavanov, A., Potter, S., Westphal, H., and Pfaff, S.L. (1998). LIM homeodomain factors Lhx3 and Lhx4 assign subtype identities for MNs. Cell *95*, 817–828.

Sockanathan, S., and Jessell, T.M. (1998). MN-derived retinoid signaling specifies the subtype identity of spinal MNs. Cell *94*, 503–514.

Storey, K.G., Crossley, J.M., De Robertis, E.M., Norris, W.E., and Stern, C.D. (1992). Neural induction and regionalisation in the chick embryo. Development *114*, 729–741.

Storey, K.G., Goriely, A., Sargent, C.M., Brown, J.M., Burns, H.D., Abud, H.M., and Heath, J.K. (1998). Early posterior neural tissue is induced by FGF in the chick embryo. Development *125*, 473–484.

Streit, A., Berliner, A.J., Papanayotou, C., Sirulnik, A., and Stern, C.D. (2000). Initiation of neural induction by FGF signalling before gastrulation. Nature *406*, 74–78.

Studer, M., Lumsden, A., Ariza-McNaughton, L., Bradley, A., and Krumlauf, R. (1996). Altered segmental identity and abnormal migration of MNs in mice lacking Hoxb-1. Nature *384*, 630–634.

Tanabe, Y., and Jessell, T.M. (1996). Diversity and pattern in the developing spinal cord. Science *274*, 1115–1123.

Tiret, L., Le Mouellic, H., Maury, M., and Brulet, P. (1998). Increased apoptosis of motoneurons and altered somatotopic maps in the brachial spinal cord of Hoxc-8-deficient mice. Development *125*, 279–291.

Tsuchida, T., Ensini, M., Morton, S.B., Baldassare, M., Edlund, T., Jessell, T.M., and Pfaff, S.L. (1994). Topographic organization of embryonic MNs defined by expression of LIM homeobox genes. Cell *79*, 957–970.

Wilson, S.I., Graziano, E., Harland, R., Jessell, T.M., and Edlund, T. (2000). An early requirement for FGF signalling in the acquisition of neural cell fate in the chick embryo. Curr. Biol. *10*, 421–429.